https://doi.org/10.1016/j.biomaterials.2018.12.020

Mussel-inspired dopamine-Cu^{II} coatings for sustained *in situ* generation of nitric oxide for prevention of stent thrombosis and restenosis

Feng Zhang[a,1], Qiang Zhang [b,1], Xiangyang Li[a], Nan Huang[a], Xin Zhao [b,]**, Zhilu Yang [a,]*

[a] Key Lab of Advanced Technology for Materials of Education Ministry, School of Materials Science and Engineering, Southwest Jiaotong University, Chengdu, 610031, China.

[b] Department of Biomedical Engineering, The Hong Kong Polytechnic University, Hung Hom, Kowloon, Hong Kong, China.

[1] Theses authors contributed equally to this work.

* Corresponding author.

** Corresponding author.

E-mail addresses: xin.zhao@polyu.edu.hk (X. Zhao), zhiluyang1029@swjtu.edu.cn (Z. Yang).

Abstract: Nitric oxide (NO) is a highly potent, yet short-lived bioactive molecule with a broad spectrum of physiological functions. Continuous and controllable *in situ* generation of NO from vascular stent surface can effectively prevent restenosis and thrombosis after its implantation. In this study, inspired by the adhesion and protein cross-linking in the mussel byssus, through immersing the stents into an aqueous solution with dopamine (DA) and copper ions (Cu^{II}), we developed a one-step metal-catecholamine assembled strategy to prepare a durable *in situ* NO-generating biomimetic coating (DA-Cu^{II}). Due to the high NO catalytic efficacy and robust chelation of Cu^{II} into the DA-Cu^{II} network, the coated stents exhibited excellent hemocompatibility. The coating also catalytically decomposed endogenous S-nitrosothiols (RSNOs) from fresh blood, and locally generated NO for over 30 days

with a flux comparable to its physiological range (0.5 - 4 × 10^{-10} mol × cm^{-2} × min^{-1}). Moreover, the optimized biomimetic coatings displayed specific cell selectivity to significantly enhance endothelial cell (EC) growth while substantially inhibit smooth muscle cell (SMC) proliferation and migration. This feature impressively promoted regeneration of a new endothelial cell layer after stent implantation, hence improved the anti-thrombogenic and anti-restenosis qualities of vascular stents *in vivo*. We envision that our long-term *in situ* NO-generating coatings could serve as biosurfaces for long-term prevention of stent thrombosis and restenosis.

Keywords: Biomimetic coating; Nitric oxide generation; Metal-catecholamine chemistry; Copper; Cardiovascular stents

1. Introduction

Cardiovascular diseases (CVDs) are a leading cause of premature death and chronic disability around the world [1]. The latest GBD (Global Burden of Disease) study on CVDs reported that there were an estimated 422.7 million cases of CVDs as well as 17.92 million CVD deaths in 2015 [1]. Currently, surgical interventional treatments with cardiovascular stents, such as bare metal stents (BMSs) and drug eluting stents (DESs), are the most common clinical therapeutic methods for treating CVDs [2]. Compared with BMSs, DESs are coated with polymers loaded with drugs, such as sirolimus and paclitaxel, which can effectively prevent neointimal hyperplasia. DESs suppress migration and proliferation of smooth muscle cells (SMCs), and remarkably reduce the incidence of in-stent restenosis to 5 - 10% [3]. However, DESs result in an incomplete and a slower re-endothelialization of the stent lumen due to multiple factors including uncontrollable drug release dosage, low biocompatibility of implanted biomaterials, activated inflammatory side effects, and simultaneous suppression on endothelial cell (EC) growth [4]. Moreover, it may lead to subsequent serious complications like late stent restenosis (LSR) and thrombosis (LST), which severely limits the stent patency rate and hampers the long-term clinical success of the interventional treatment [5].

To mitigate these clinical problems, considerable efforts have been made in the last decade to develop cardiovascular stents with improved safety and efficacy [6]. Stent surface modifications by coating with biomolecules such as adhesive peptides [7, 8], vascular endothelial growth factors (VEGFs) [9] and nitric oxide (NO)-releasing/generating molecules [10-12] have been proposed as a one effective solution. Apart from preserving the adequate mechanical properties of the stent to prevent constrictive vascular remodeling, surface modification strategies can further improve the hemocompatibility of stents through the behavioral regulation of platelets, ECs and SMCs [3, 13]. Among these biomolecules, NO, which is a small but highly potent signaling molecule synthesized and secreted by ECs, plays the most critical role in several physiological processes including anti-atherogenesis, vasodilation, stimulation of EC growth, inhibition of SMC proliferation, and platelet activation/aggregation [14, 15]. In various animal models, NO-releasing or -generating surface modifications exhibit greatly improved anti-thrombotic and anti-restenosis efficacy, and are thus highly sought after [4, 16, 17]. However, in stoichiometric NO-releasing coatings, most NO donors such as RSNOs and N-diazeniumdiolates are fragile because they are liable to spontaneous decomposition upon exposure to heat, moisture or light [18, 19]. In addition, unlike healthy ECs, which can sustainably generate a high cumulative amount of NO at a low level ranging from 0.5 - 4 × 10^{-10} mol × cm^{-2} × min^{-1}, these donors can only release a limited amount of NO only for a short time period [11]. For these reasons, the NO-releasing coatings are unable to effectively alleviate late complications after stent implantation and are not suitable for long-term implantations. Moreover, NO in human blood is short-lived (approximately 1.8 s) and can only diffuse over a very short distance (approximately 100 μm) to exert its biological functions [20, 21]. Therefore, to endow the implanted stent with the ability to prevent LSR and LST, strategies for sustained and site-specific generation of NO on the stent surface are highly desirable.

To generate NO in a controllable manner, our group previously adopted various glutathione peroxidase (GPx)-like catalytic mimics (i.e., selenocystamine and 3,3-diselenodipropionic acid) to develop NO-generating coatings [22-24]. These catalytic

coatings took advantage of the endogenous NO donors (i.e., RSNOs) from the circulating blood for a stable and sustainable generation of NO at the blood/stent interface. To further improve the catalytic efficacy of the surface coatings, we propose a strategy in the present study that employs copper (Cu) ions, which are a transition metal ion with excellent GPx-like NO catalytic activity [25], to fabricate a biomimetic NO-generating coating. In addition, Cu is also an angiogenesis stimulus that promotes the recruitment and differentiation of blood cells by enhancing VEGF and hypoxia-inducible factor expressions, which is beneficial for wound healing [26]. In order to immobilize the Cu ions onto a stent surface, we put forward a one-step metal-catecholamine assembling strategy to form DA-Cu^{II} coordination complexes on cardiovascular stent surfaces. This facile surface engineering strategy is inspired by the adhesion and protein cross-linking chemistry of [$Fe(DA)_3$] complexes found in mussel byssus coatings (**Fig. 1**A (i-iii)). To the best of our knowledge, it is the first report of such functional cardiovascular stent coatings combining *in situ* NO catalysis of Cu^{II} with excellent surface properties of DA. Such Cu-containing coatings exhibit admirable biocatalytic performances which enables continuous, controllable and local conversion of endogenous RSNOs to active NO. As a result, it significantly enhances EC functions, and effectively inhibits SMC migration and proliferation. More importantly, it ultimately promotes re-endothelialization and prevents LSR and LST. Due to the simplicity and availability of conjugating DA onto various material surfaces regardless of their complicated shapes, we envision that this strategy can be further extended to modify different blood-contacting surfaces for other biomedical applications.

2. Materials and methods

2.1. Preparation of DA-Cu^{II} coatings

Dopamine hydrochloride at a constant concentration of 0.25 mg/mL was firstly dissolved by 10 mM Tris-HCl (pH 8.5). Afterwards, $CuCl_2 \cdot 2H_2O$ at concentrations of 0, 1, 2.5, 5, 7.5 and 10 μg/mL were added separately. In order to form DA-Cu^{II} coatings onto the planar substrate, 316L SS planar substrate (10 mm × 10 mm) was dipped into the above mixed solution. After dip-coating for 12 h at room temperature, the coated

samples were ultrasonically rinsed with distilled water to remove potential debris on the surfaces, and were dried under N_2 gas. To prepare DA-Cu^{II} coatings onto cardiovascular stents, 0.25 mg/mL dopamine hydrochloride and 5 μg/mL $CuCl_2 \cdot 2H_2O$ were selected as the reaction solutions for 316L stainless steel (SS) stent (Φ1.65 mm × 18 mm) surface engineering. The procedures of dip-coating cardiovascular stents and washing were similar as described above.

2.2. Characterization of DA-Cu^{II} coatings

The surface morphology and roughness were analyzed by the atomic force microscope (AFM, Bruker, Germany) using tapping mode configuration. Furthermore, the coating thickness was measured with a spectroscopic ellipsometer (M-2000V, J.A. Woollam, USA). Wavelengths from 370 to 1000 nm were used to measure the Δ and Ψ values, and a Cauchy model was applied to determine the coating thickness. The hydrophilicity alteration of the sample surface after dip-coating was examined by measuring water contact angles (WCAs) of the coating with a Krüss GmbH DSA 100 Mk 2 goniometer (Hamburg, Germany) at room temperature. Six different measurement sites in each sample were chosen at random. The surface elemental composition of NO-generating coatings was analyzed by X-ray photoelectron spectroscopy (XPS). In this study, two instruments of XPS were used. One of the instruments (XSAM800, Kratos Ltd, UK) was equipped with a monochromatic Al Kα (1486.6 eV) X-ray source operated at 12 kV × 15 mA and a pressure of 2×10^{-7} Pa. Moreover, the C1s peak (binding energy 284.8 eV) was used as a reference for charge correction. The full-width at half-maximum (fwhm) value of 1.9 ± 0.2 eV was taken equally for all the components and was determined by a gold standard. The overview XPS spectra was taken between 50 and 1300 eV with an energy step of 0.5 eV using a pass energy of 300 eV, while the detailed spectra peaks of interest were recorded with an energy step of 0.05 eV. The total acquisition time was 15 min for each sample. Electron paramagnetic resonance (EPR) measurement was performed on an A320 apparatus (Bruker, Germany) to evaluate the effect of DA-Cu^{II} coordination on coating network formation. In addition, the matrix assisted laser desorption ionization mass spectrometry (MALDI MS) was

measured with a MALDI micro MX time-of-flight mass spectrometer (Waters, Milford, MA) in order to investigate the chemical structure of DA-Cu^{II} coating. The detailed operation and analysis process were reported elsewhere [24, 27].

2.3. Mechanical tests of DA-Cu^{II} coatings

To assess the mechanical properties of DA-Cu^{II} coatings on the stents, a balloon dilatation test was performed. Firstly, the bare 316L SS cardiovascular stents were modified with DA-Cu^{II} coatings, and then mounted onto angioplasty balloons by stent crimpers. After dilating the balloon to a diameter of 3 mm at a pressure of 9 atm for 1 min, field emission scanning electron microscopy (FE-SEM, JSM-6390, JEOL, Japan) was used to investigate the surface morphology of the post-expansion stents.

2.4. NO catalytic generation from the DA-Cu^{II} coatings

Real-time monitoring of NO generation induced by DA-Cu^{II} coatings was carried out with a chemiluminescence NO analyzer (Seivers 280i, Boulder, CO). In this study, DA-Cu^{II} coatings were prepared onto the 316L SS foil (0.5 cm × 1 cm). The NO was catalytically generated from the DA-Cu^{II} coatings by immersing samples into a 5 mL test phosphate buffered saline (PBS, pH 7.4) solution, which contains 10 μM NO donor S-Nitrosoglutathione (GSNO, one of the most typical endogenous RSNO species used for NO release test) and 10 μM of reducing agent glutathione (GSH) at 37^{o}C for about 40 min. Then, the generated NO was transported to a chemiluminescence NO analyzer under a continuous stream of N_2 gas. The amount of NO induced by the DA-Cu^{II} coatings was then calculated according to the calibration curves of the NO analyzer [28]. To further investigate the long-term catalytic effect of the DA-Cu^{II} coatings, the coated 316L SS foils were immersed into the test PBS solution containing the NO donor (10 μM GSNO and 10 μM GSH), which was replaced every 12 h, at 37^{o}C for 1, 5, 10, 15 and 30 days respectively. Then, the NO donor treated samples were tested for NO catalytic efficacy following similar steps as described above.

2.5. Adhesion and proliferation of human umbilical vein endothelial cells (*HUVECs*)

To simulate the *in vivo* environment of a cardiovascular system, the growth behaviors of HUVECs on the DA-Cu^{II} coatings were investigated. The HUVECs were seeded on the sample surface at an initial density of 5×10^4 cells/cm^2. Then, the cells were cultured in the culture medium containing NO donor (10 μM GSNO and 10 μM GSH), and the NO donor was supplemented every 6 h. After incubation for 2, 24 and 72 h at 37°C under 5% CO_2 respectively, the samples were gently taken out under aseptic conditions and the cells on the sample surfaces were subsequently stained with phalloidin conjugated tetramethyl rhodamine. Instructions provided by the manufacturer were strictly followed in order to accurately analyze the adhesion and spreading behaviors of the cells. Furthermore, proliferation of the cells cultured on the surfaces for 24 and 72 h were evaluated with Cell Counting Kit-8 (CCK-8) [29].

2.6. Function evaluation of HUVECs

For the evaluation of functional expression of ECs, 1 mL HUVECs suspension with 1×10^5 cells was added to each sample and cultured for 24 h. Then, 0.1% triton X-100 and 10 mg/mL phenylmethanesulfonyl fluoride (PMSF) were added for 10 min while samples were placed on an ice-water bath. The pyrolysis solution was collected and centrifuged at 10000 rpm for 10 min at 4 ^oC. Then, the supernatant fluid was collected for the detection of plasminogen activator inhibitor (PAI), tissue plasminogen activator (tPA), von Willebrand factor (vWF) and prostaglandin I_2 (PGI_2) via ELISA assay kits according to the attached instructions.

2.7. Adhesion and proliferation of human umbilical artery smooth muscle cells (*HUASMCs*)

Similar to HUVEC assay, HUASMCs were also seeded onto the sample surfaces at a density of 5×10^4 cells/cm^2 for 2, 24 and 72 h respectively. For the first 24 and 72 h of the culture, NO donor (10 μM GSNO and 10 μM GSH) was supplemented every 6 h. The morphology and proliferation of HUASMCs were detected via phalloidin staining and CCK-8, respectively [29].

2.8. Migration of HUVECs and HUASMCs

To mimic the natural situation of ECs and SMCs in blood vessels, HUVECs or HUASMCs were seeded onto a sample surface at a density of 5×10^5 cells/cm^2 and incubated for 6 h in order to form a complete cell layer on the surface. Briefly, the 316L SS foils with a size of 15 cm × 10 cm were first vertically folded in half, and were then immersed halfway into the reaction solution to form a DA-Cu^{II} thin film on one flank. Subsequently, HUVECs or HUASMCs were seeded onto another untreated flank of all 316L SS foils. After culturing for 6 h, all samples were vertically turned over and transferred onto a new well plate so that the DA-Cu^{II}-coated flank was immersed into the fresh culture medium with NO donor supplemented every 6 h. After one day of continuous incubation, the samples were then washed with saline solution, and fixed with glutaraldehyde (2.5%) prior to phalloidin staining. Ultimately, the migration behavior of HUVECs or HUASMCs was observed and photographed by a Leica DMRX fluorescence microscope.

2.9. Co-culture of HUVECs and HUASMCs

To investigate the competitive adhesion and proliferation behaviors of HUVECs and HUASMCs, both types of cells were co-cultured on the stent surfaces. In order to mark the different cells, HUVECs and HUASMCs were pre-labeled in different colors with different cell trackers. HUVECs were labelled with green chloromethyl fluorescein diacetate (CMFDA), while HUASMCs were labelled with orange chloromethyl trimethyl rhodamine (CMTMR) under product instructions (Molecular Probes/ThermoFisher, Oregon, USA). Then, the labelled HUVECs and HUASMCs were digested by a trypsin-EDTA solution (0.25% wt) prior to being centrifuged at 1200 rpm for 5 min. After re-suspension in the DMEM/F12 medium with 10% fetal bovine serum (FBS), a suspension solution of each cell type at a concentration of 5×10^4 cells/mL was obtained separately. Finally, both types of cell suspensions were mixed at a volume ratio of 1:1 and added to the samples at a density of 5×10^4 cells/cm^2. After co-culturing for 2 and 24 h in a cell incubator at 37°C under 5% CO_2, the cells

were observed and photographed by a Leica DMRX fluorescence microscope. Twelve images were used to count the number of attached cells via Image J software.

2.10. Anti-thrombogenicity test by ex vivo blood circulation

All animal handling and surgical procedures were in agreement with the China Council on Animal Care, and the protocols used were approved by the Animal Ethics Committee of Southwest Jiaotong University. The experimental procedures were similar to those described in our previous studies [24, 30]. Six New Zealand white rabbits weighing 2.5 ~ 3.5 kg were chosen for the rabbit extracorporeal circuit model experiment. The left carotid artery and the right jugular vein of the rabbits were firstly isolated under general anesthesia, and were then connected with tubes to form an arteriovenous (AV) shunt. In this work, the uncoated and DA-Cu^{II}-coated 316L SS foils (0.8 mm × 1 mm) were curled and tightly assembled onto the inner wall of polyvinyl chloride (PVC) tubes (a kind of commercially available cardiopulmonary perfusion tube). After that, the assembled tube was integrated into the rabbit AV-shunt and remained running for 2 h with supplement of NO donor (0.0111 μmol/kg/min of the GSNO and 0.0111 μmol/kg/min of the GSH) into the blood. Cross sections of the tubes were photographed for analyzing their percent occlusion. The residual clots in the tube around the implanted samples were collected, photographed and weighted. The samples were removed, washed with PBS and fixed with glutaraldehyde solution (2.5%) overnight. After being dehydrated, dealcoholized and dried, all samples were finally inspected with SEM.

2.11. In vivo stent implantation

Eight healthy New Zealand white adult rabbits (3.5 ~ 4.0 kg) and 16 cardiovascular stents were used in this experiment. The rabbits were divided into two groups: the control uncoated 316L SS stents group and the DA-Cu^{II} coated 316L SS stents group. After general anesthesia, two stents from each group were implanted into the left and right iliac arteries of the rabbit. The rabbits were then sacrificed at time points of 1 and 3 months (n = 4 for each time point) before the post-implantation stents were taken out

for analysis. The angiography under anesthesia was performed to confirm the patency of the iliac artery following the implantation of 1 and 3 months. Half of the stented arteries were snipped lengthwise and fixed with glutaraldehyde (2.5%) in PBS. After being dehydrated, dealcoholized and critical point dried, these stented arteries were observed using SEM. The other half of the stented arteries were fixed with formaldehyde (10%) in PBS for 2 days, and were then stained with Van Gieson's stain for histomorphometric examination.

2.12. Statistical analysis

All materials, cells, *ex vivo* and *in vivo* experiments were performed independently at least in quadruplicate for statistical significance. The results of the experiments were expressed as mean ± standard deviation (SD). Data analysis was performed by one-way analysis of variance (ANOVA), and a p value of less than 0.05 was considered statistically significant.

3. Results and discussion

3.1. Characterization of DA-Cu^{II} coatings

The DA-Cu^{II} coatings on the 316 L SS surface (one of the most common biomaterials for cardiovascular stents [31]) were prepared by one-step dip-coating of the samples into an alkaline aqueous solution (pH 8.5), that contains Cu^{II} ions and DA. To obtain NO-generating coatings with adjustable and controllable release rates, DA-Cu^{II} coatings produced by immersing samples into various $CuCl_2 \cdot 2H_2O$ feed concentrations of 0, 1, 2.5, 5, 7.5 and 10 μg/mL were evaluated. After 12 h of immersion, the 316L SS substrates displayed a polydopamine-like brown color (**Fig. 1**B). AFM images confirmed the presence of DA-Cu^{II} thin coatings on the 316 L SS surface (**Fig. S1**) with coating thickness ranging from 18.4 to 28.6 nm, as indicated by the spectroscopic ellipsometer (**Fig. 1**C). WCA analysis also confirmed the success of the surface coatings on the 316 L SS surface (**Fig. S2**). The unmodified 316L SS substrates presented a WCA value of 75.0 ± 2.9°, and was sharply reduced to 35 - 43° after deposition with DA-Cu^{II} coatings, probably attributed to the introduction of hydrophilic

DA [32]. To further understand the surface chemical compositions, the coatings were characterized by XPS. The presence of a new peak of Cu2p (~934 eV) of the coated surface revealed a successful chelation of Cu ions (**Fig. S3**). Moreover, as shown in **Fig. 1**D, the content of the Cu in the DA-Cu^{II} coatings was proportional to the feed concentrations of $CuCl_2 \cdot 2H_2O$ (**Table S1**), indicating that we can adjust the distribution of Cu in the DA-Cu^{II} coatings simply by changing the feed concentration of $CuCl_2 \cdot 2H_2O$.

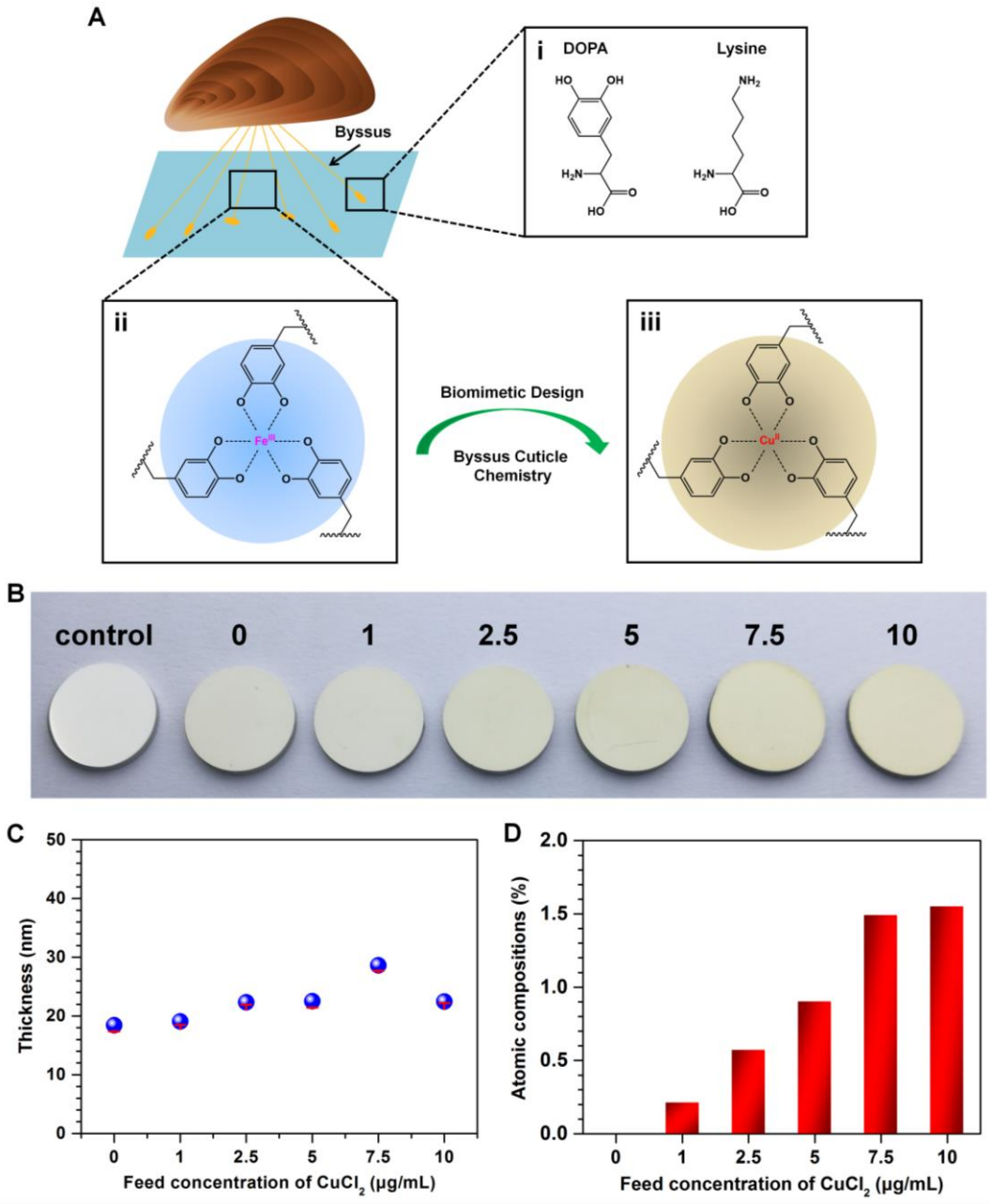

Fig. 1. Formation and characteristics of DA-Cu^{II} coatings**.** (A) Mussel-inspired adhesive and cross-linking strategy for Cu^{II} coating: (i) Schematic displaying a mussel

strongly adhering to a wet surface by secreting a bundle of threads called byssus. Reactive catechol-containing compound Levo-DA (L-DA) and lysine are the two key residues for mussel adhesion and curing. (ii) The catechol moieties of L-DA in byssus form strong tris [$Fe(DA)_3$] complexes to crosslink mussel foot protein 1 (mfp-1). (iii) Bio-inspired by the adhesion and cross-linking chemistry of the Fe^{III} complexes, DA and Cu^{II} are chosen to form DA-Cu^{II} thin films on stent surfaces to immobilize the Cu^{II} catalyst. (B) Control 316L SS substrates before and after modification with DA-Cu^{II} coatings, which were prepared with different feed concentrations of $CuCl_2 \cdot 2H_2O$ ranging from 0 to 10 μg/mL. (C) Thickness of DA-Cu^{II} coatings. (D) Atomic compositions of copper in DA-Cu^{II} coatings.

Next, we used EPR spectroscopy to demonstrate the contribution of DA-Cu^{II} coordination on the coating network formation. Aqueous suspensions of control uncoated, DA-coated and DA-Cu^{II}-coated samples were introduced into an EPR tube to test for the presence of paramagnetic species. It was found that the spectrum of DA-Cu^{II}-coated samples showed a broad Cu-related signal at 3440 mT (**Fig. 2**A), indicating the formation of a DA-Cu^{II} coordination network. To further understand the possible polymerization process of the DA-Cu^{II} coatings, MALDI MS analysis was performed. The successful immobilization of DA onto the surface was demonstrated by peaks at 685, 523 and 409 m/z. For DA-Cu^{II} coating synthesis, the introduction of Cu^{II} significantly influenced the self-polymerization manner of DA. The possible crosslinking reaction between the Cu^{II} and DA was mainly based on the catechol-metal coordination chemistry to form bis- and tris-catechol-Cu^{II} complexes, as demonstrated by the clear presence of peaks at 362 and 511 m/z (**Fig. 2**B and C). Overall, the above results demonstrated that the 316L SS substrate was successfully modified with a thin film of DA-Cu^{II} coordination complexes.

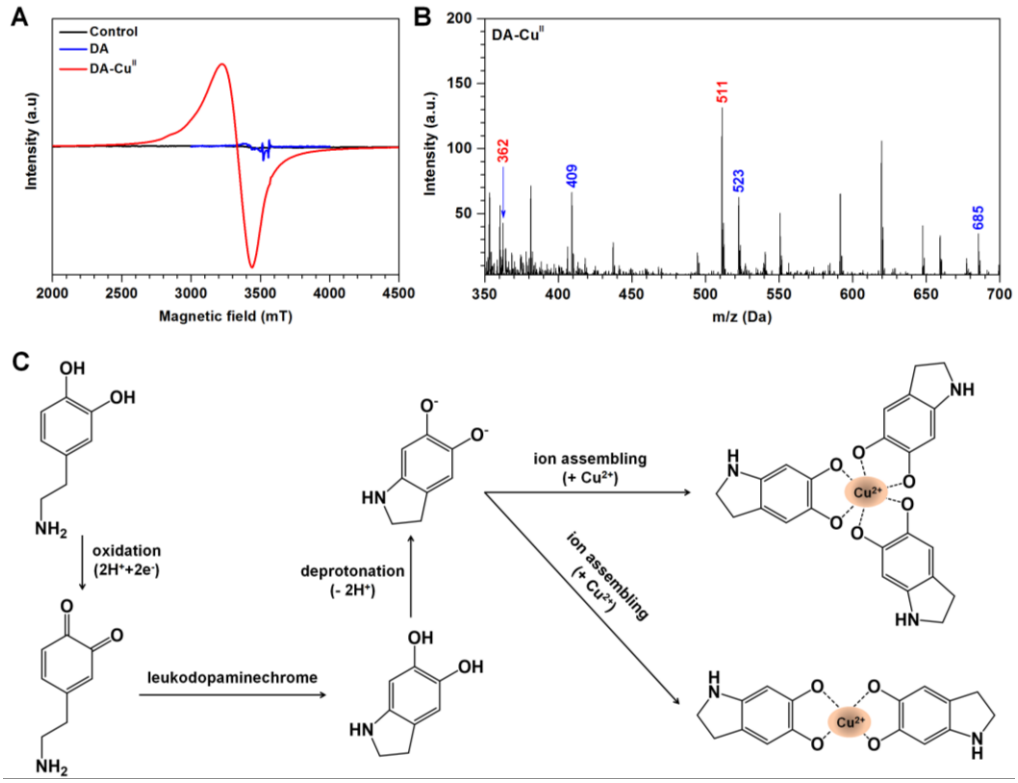

Fig. 2. EPR spectra and MALDI MS analysis of the DA-Cu^{II} coatings. (A) EPR spectra of uncoated control, DA-coated and DA-Cu^{II}-coated samples. (B) MALDI MS analysis of the DA-Cu^{II} complexes (red peak represents Cu^{II}, blue peak represents DA). (C) Possible chemical reactions between Cu^{II} and DA.

3.2 In vitro evaluation of catalytic NO generation from the DA-Cu^{II} coatings

NO is an important signaling molecule associated with several critical vascular physiological processes, such as maintaining vascular homeostasis as well as acting as a potent vasodilator [14]. Although gaseous NO is short-lived (approximately 1.8 s) and has low generation rates from the healthy endothelial layer ($0.5 - 4 \times 10^{-10}$ mol × cm^{-2} × min^{-1}), a deficiency of NO production or a reduction in its bioavailability is associated with intimal hyperplasia and thrombosis formation [20, 33]. Therefore, a long-term, continuous, and stable release of NO from the surface of biomedical devices is crucially important for the sake of cardiovascular tissue engineering.

As previously mentioned, transition metals such as Cu are able to catalytically initiate NO release from both endogenous and synthetic RSNOs via decomposing RSNOs in the presence of reductant GSH [19, 34]. We thus believe that the

incorporation of Cu^{II} into cardiovascular stents for long-term localized supplement of NO would be a feasible method to alleviate LSR and LST. In this work, NO catalytically generated under physiological pH from the DA-Cu^{II} coatings was evaluated via a chemiluminescence-based NO analyzer. As shown in **Fig. 3**A and B, real-time monitoring of NO generation revealed that the DA-Cu^{II} coatings exhibited a stable and dose-dependent manner of Cu^{II} immobilization: by increasing the feed concentration of $CuCl_2 \cdot 2H_2O$ from 1 to 10 μg/mL, the NO release rates can be modulated from 0.4 to 6.5 × 10^{-10} mol × cm^{-2} × min^{-1}, which are comparable to the physiological level of the NO synthesis rate (0.5 - 4 × 10^{-10} mol × cm^{-2} × min^{-1}). Such differences in the NO release rate may be attributed to the higher catalytic ability of Cu^{II} at the higher feed concentration of $CuCl_2 \cdot 2H_2O$ [19, 34, 35]. In addition, after continuous immersion in PBS solution for 30 days, the NO flux of the DA-Cu^{II} coatings (5 μg/mL $CuCl_2 \cdot 2H_2O$) decreased slightly, but still remained as high as 3.8 × 10^{-10} mol × cm^{-2} × min^{-1}, representing 72% of the NO generation rate of the initial DA-Cu^{II} coatings (**Fig. S4**). XPS analysis of the DA-Cu^{II} coating after 30 days of immersion in PBS solution revealed a high retention of approximately 69% in the initial content of copper (**Fig. S5, Table S2**). These results suggested that our coatings demonstrated an excellent long-term (30 days) stability for NO catalytic activity, which clearly outcompetes other existing platforms that usually provide limited NO gas and show a substantial reduction in the NO release rate as time progresses [24, 36]. Consequently, our DA-Cu^{II} coatings can be concluded to possess the ability to produce a controllable, stable and durable release of NO flux, with a potential long-term therapeutic efficacy as coatings for blood-contacting devices.

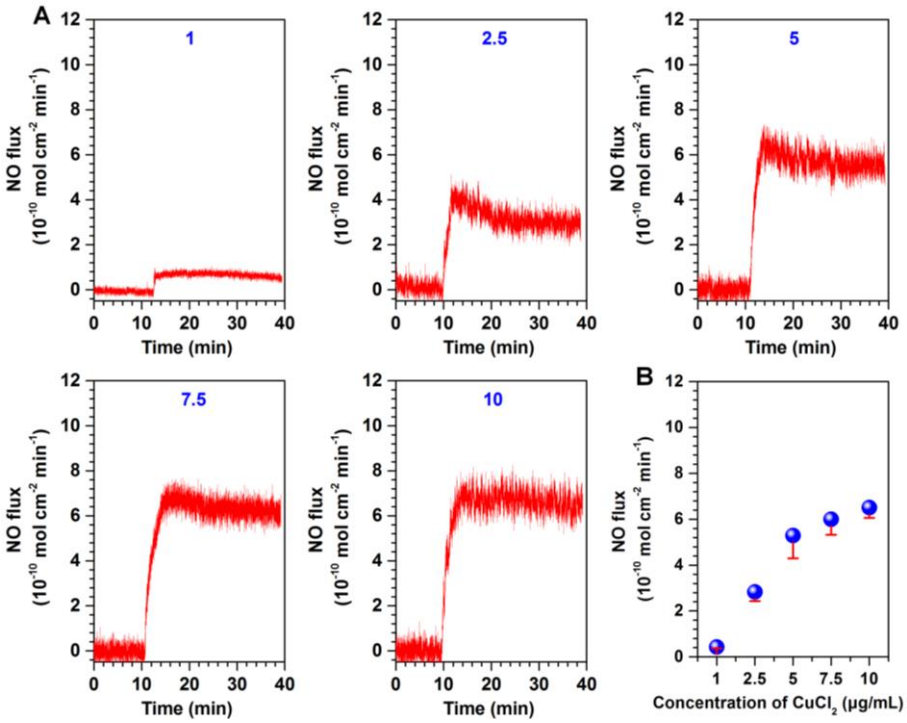

Fig. 3. Catalytic NO generation from the DA-Cu^{II} coatings. (A) Catalytic NO generation patterns of various samples prepared at different feed concentrations of $CuCl_2 \cdot 2H_2O$ (1, 2.5, 5, 7.5 and 10 μg/mL) in PBS consisting of NO donor (10 μM GSNO and 10 μM GSH). (B) Calculated release rates of NO induced by different DA-Cu^{II} coatings.

3.3 Effects of DA-Cu^{II} coatings on growth behavior of ECs and SMCs

The interactions of vascular cells, such as ECs and SMCs, with the surrounding microenvironment provided by the biomaterials are pivotal in determining the ultimate functionality of implanted blood-contacting devices [37]. It has been frequently demonstrated that a rapid regeneration of healthy EC layer on the cardiovascular stent surfaces after implantation alleviates the issues of LSR and LST [37, 38]. Therefore, it is important to know how ECs respond to DA-Cu^{II} coatings. Firstly, we cultured the HUVECs on the DA-Cu^{II} coatings either with or without presence of NO donor in a culture media, and investigated the effects of coatings on cell adhesion, proliferation and migration (**Fig. 4**). In the group without donor supplements, the HUVECs on all DA-Cu^{II} coatings showed slightly improved adhesion after 2 h of culture. Another important detail to note was that the cell growth was enhanced after 24 and 72 h of

culture when compared with the control 316L SS. It indicated that the DA-Cu^{II} coatings offered a better microenvironment to support cell growth (**Fig. 4**A and B). This was most likely due to the introduction of positively charged amine groups and Cu content on the coating surfaces [26, 32]. When we added the donor supplement to the medium, the DA-Cu^{II} coatings on average displayed a significantly enhanced adhesion and proliferation effect of HUVECs compared to the control 316L SS due to the presence of NO produced by the DA-Cu^{II} coatings (**Fig. 4**A and C). We also found that if the feed concentration of $CuCl_2 \cdot 2H_2O$ for the coating exceeded 5.0 μg/mL, the resultant DA-Cu^{II} coating slightly inhibited HUVEC proliferation, possibly due to the high concentration of generated NO (excessive amount of NO may produce peroxynitrites ($ONOO^-$), an undesirable compound for stent re-endothelialization *in vivo* [39]). Physiological function of ECs grown on the vascular stents is as important as cell adhesion and proliferation. Therefore, based on the evaluation of cell adhesion and proliferation, we further evaluated some of the functional molecules secreted by ECs cultured on the previously mentioned surfaces with/without NO donor, namely vWF, PAI, tPA, and PGI2 via ELISA. The results revealed that the DA-Cu^{II} coatings, whether in the group supplemented with NO donor or without NO did not seem to sacrifice the normal function of ECs, because there was no significant difference in the secretion of all the functional molecules between the bare 316L SS and DA-Cu^{II} coated surfaces (**Fig. S6**). This indicated the good biocompatibility of the DA-Cu^{II} used as stent coating.

In addition, as promoted EC migration from adjacent natural endothelia to stents plays a vital role in the *in situ* re-endothelialization after implantation, we further performed a cell migration assay. We found that the DA-Cu^{II} coating (5 μg/mL $CuCl_2 \cdot 2H_2O$ was chosen for fabrication of coating for the cell migration assay based on the results of HUVEC proliferation) also enhanced HUVEC migration in the group without NO donor. After supplementing the NO donor in the cell media, the DA-Cu^{II} coating showed further enhancement in HUVEC migration due to the physiological effect of NO generated by the coatings (**Fig. S7**).

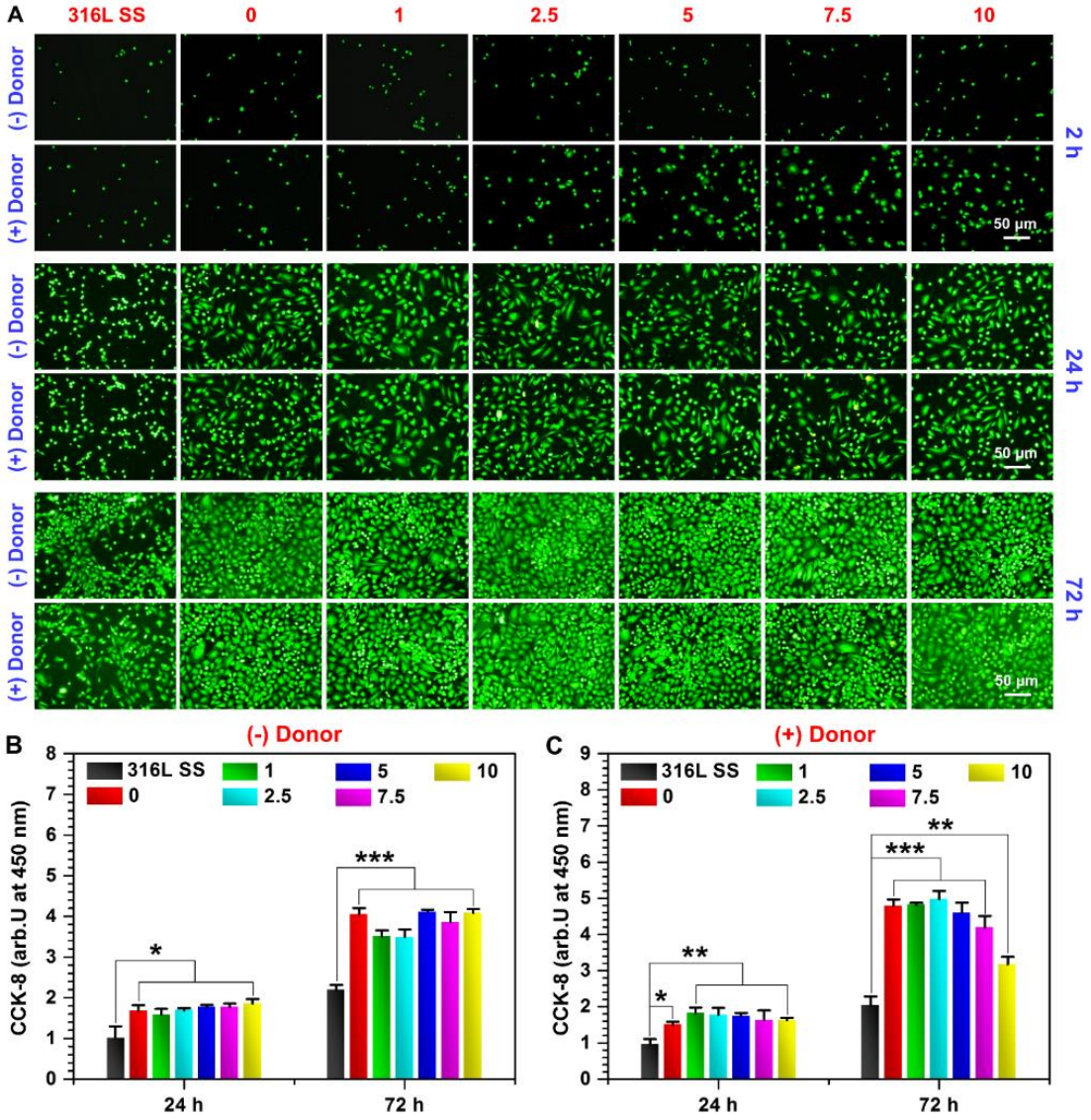

Fig. 4. Adhesion and proliferation of HUVECs cultured on different samples. (A) Fluorescence staining of HUVECs incubated in cell culture media with and without NO donor (10 μM GSNO and 10 μM GSH) for 2, 24 and 72 h, respectively. Proliferation analysis of HUVECs incubated in cell media (B) without and with (C) NO donor for 24 and 72 h. Data are presented as mean ± SD and analyzed by one-way ANOVA (n = 4, *p < 0.05, **p < 0.01, and ***p < 0.001).

Vascular SMCs promote neointimal hyperplasia through cellular expansion and extracellular matrix deposition [4]. Therefore, the inhibition of its adhesion, proliferation and migration is crucial to reduce the risk of LSR. Thus, the responses of HUASMCs to the DA-Cu^{II} coatings were also further investigated in addition to

HUVECs. As shown in Fig. 5A and B, in the absence of the NO donor, HUASMCs grew well on 316L SS and all DA-Cu^{II} coated surfaces. However, for the group supplemented with NO donor, the adhesion and growth of HUASMCs on the DA-Cu^{II} coatings were substantially inhibited (**Fig. 5**A and C). In addition, it was noteworthy that the inhibitory effect on the HUASMCs could be further enhanced with a higher concentration of $CuCl_2 \cdot 2H_2O$. This implies that an increase in chelation of the Cu^{II} in the DA-Cu^{II} coatings improved the bioavailability and bioactivity of NO by increasing its catalytic ability (**Fig. 5**C). In the subsequent migration assay of SMCs, we found that the migration rate of HUASMCs on the DA-Cu^{II} coating (5 μg/mL $CuCl_2 \cdot 2H_2O$) without presence of the NO donor was slightly reduced as compared to the 316L SS. Nevertheless, we observed a remarkable decrease in the migration behavior of HUASMCs in the DA-Cu^{II} coatings (with a dramatic decrease of 250% in the migration distance) in the presence of the NO donor (**Fig. S8**). The data acquired suggested that our DA-Cu^{II} coatings could effectively discourage attachment, migration and proliferation of HUASMCs, with a great potential for suppressing intimal hyperplasia and following stenosis.

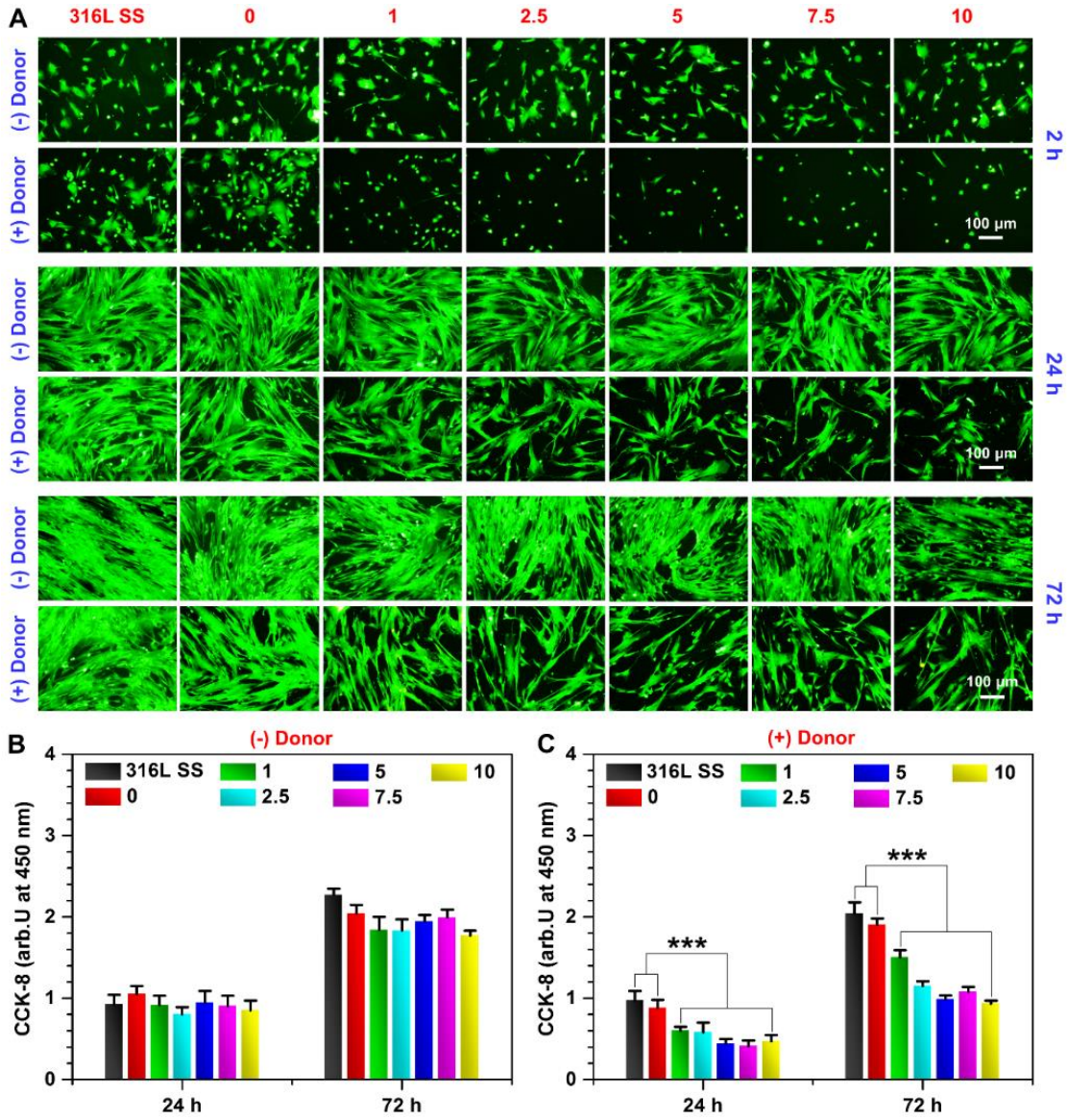

Fig. 5. Adhesion and proliferation of HUASMCs cultured on different samples. (A) Fluorescence staining of HUASMCs incubated in cell culture media with and without NO donor (10 μM GSNO and 10 μM GSH) for 2, 24 and 72 h, respectively. Proliferation analysis of the HUASMCs incubated in cell media (B) without and with (C) NO donor for 24 and 72 h. Data are presented as mean ± SD and analyzed by one-way ANOVA (n = 4, ***p < 0.001).

Many studies have demonstrated that competitive adhesion and growth of ECs and SMCs *in vivo* are also crucial for the formation of a new yet pure EC layer on a stent surface as well as the prevention of LSR and LST [23, 40, 41]. To evaluate the competitive behaviors between ECs and SMCs on the DA-Cu^{II} coatings, HUVECs and

HUASMCs were co-seeded onto the surfaces of various samples at a ratio of 1:1. After co-culturing for 2 h, the result of competitive adhesion demonstrated that the ratio of HUVECs to HUASMCs in the 316L SS sample was 0.52 ± 0.07, slightly lower than that in most of the DA-Cu^{II}-coated samples (**Fig. 6**A and B). Following the addition of the NO donor to the culture medium, a notable increase in the amount of HUVECs and a decrease in the HUASMCs were observed, especially in the DA-Cu^{II} coatings which had a high Cu^{II} content (**Fig. 6**A and C). Similarly, in the absence of the NO donor, cell growth on the 316L SS and DA-Cu^{II} coatings showed no significant difference after 24 h of culture. In contrast, the amount of HUVECs grown on the DA-Cu^{II}-coated surfaces remarkably increased after the addition of NO donor, whereas the amount of HUASMCs was dramatically reduced (**Fig. 6**). The competitive adhesion and growth advantages of HUVECs over HUASMCs on the DA-Cu^{II} coatings achieved via catalytic generation of NO suggested the potential in forming an endothelial layer on stents *in vivo*.

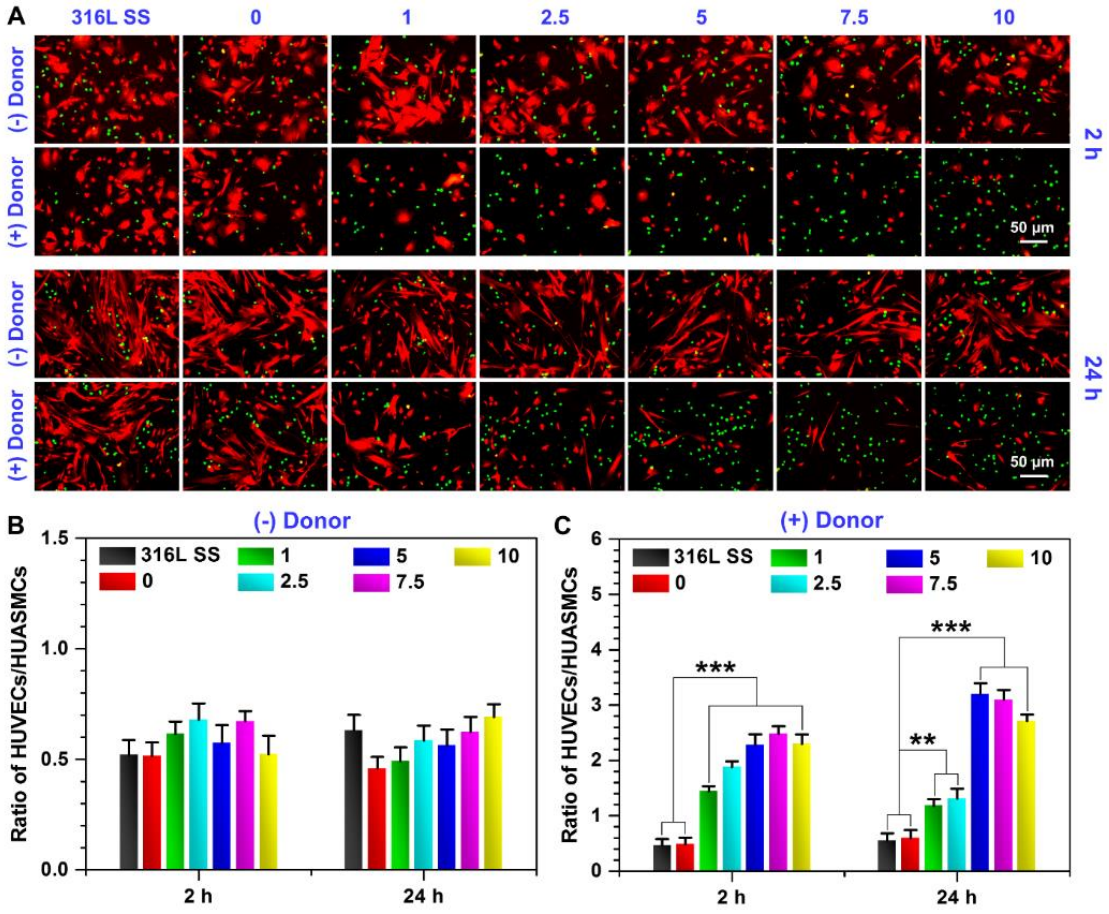

Fig. 6. Competitive adhesion between HUVECs and HUASMCs on the uncoated and DA-Cu^{II}-coated 316L SS stents after culture for 2 and 24 h. (A) Fluorescence staining of HUVECs using CMFDA (green) and HUASMCs using CMTMR (red). The ratio of HUVECs/HUASMCs grown on the different stent surfaces (B) without and (C) with the addition of NO donor (10 μM GSNO and 10 μM GSH) into the cell culture media. Data are presented as mean ± SD and analyzed by one-way ANOVA (n=6, **$p < 0.01$ and ***$p<0.001$).

Overall, the above results implied that the DA-Cu^{II} coatings could endow the cardiovascular stents with the ability of long-term *in situ* NO generation to improve re-endothelialization by selectively promoting EC attachment, proliferation and migration. At the same time, they potentially reduced LSR and LST risks by suppressing SMC attachment, proliferation and migration. Based on the above systematic *in vitro* evaluation, the NO-generating DA-Cu^{II} coatings formed by immersion in 5 μg/mL $CuCl_2 \cdot 2H_2O$ showed the most desirable NO generation and biological effects (i.e., enhanced growth and migration of HUVECs and reduced adhesion and proliferation of HUASMCs). For this reason, 5 μg/mL of $CuCl_2 \cdot 2H_2O$ has been selected to engineer stent surface for the subsequent *ex vivo* and *in vivo* evaluation.

3.4 Ex vivo anti-thrombogenic property of the DA-Cu^{II} coatings

An arteriovenous shunt (AV-shunt) assay was employed to obtain further insight into the anti-thrombogenic properties of the DA-Cu^{II} coatings under the actual blood flow using a rabbit extracorporeal circuit model (**Fig. 7**A). After 2 h of circulation, there was only little wall clot in the perfusion tube with internal installation of the DA-Cu^{II} coated 316L SS foil compared to that of the naked 316L SS foil (**Fig. 7**B and C). The correlated statistical analysis of the occlusion exhibited that the naked 316L SS foils had a considerably high percent occlusion of 89.5 ± 7.5 %, whereas no distinct occlusion was detected in the DA-Cu^{II} coated samples (**Fig. 7**D). Moreover, the DA-Cu^{II} coated 316L SS foils also possessed substantially reduced weight in the formed thrombus compared to the naked 316L SS foil, 38.2 ± 5.5 mg and 1.1 ± 0.2 mg, respectively (**Fig. 7**E). To

further understand the influences of the DA-Cu^{II} coatings on platelet adhesion, surface morphology of the samples was analyzed with SEM after 2 h of blood circulation. The results indicated that the number of adhered platelets and formation of fibrin deposited on the DA-Cu^{II} coated surfaces significantly decreased when compared to that on the 316L SS control group, possibly due to the reduced formation of thrombus (**Fig. 7**F). In addition, as undisturbed blood flow in the tube of the implanted cardiovascular stent is another essential characteristic of hemocompatibility, we then analyzed the blood flow data of different circuits during the *ex vivo* AV-shunt assays. We found that the blood flow rate of all circuits decreased to different degrees at the end of extracorporeal circulation experiments compared to the initial value **(Fig. 7**G). However, the blood flow rate in circuits with the DA-Cu^{II} coated 316L SS foil still remained noticeably high at 91.3 ± 5.4%. On the other hand, an approximate decrease of 78% was observed from the circuits with naked 316L SS foil. All in all, these *ex vivo* results ascertained an improved hemocompatibility of blood-contacting devices when using our DA-Cu^{II} coatings to continuously generate NO *in situ*.

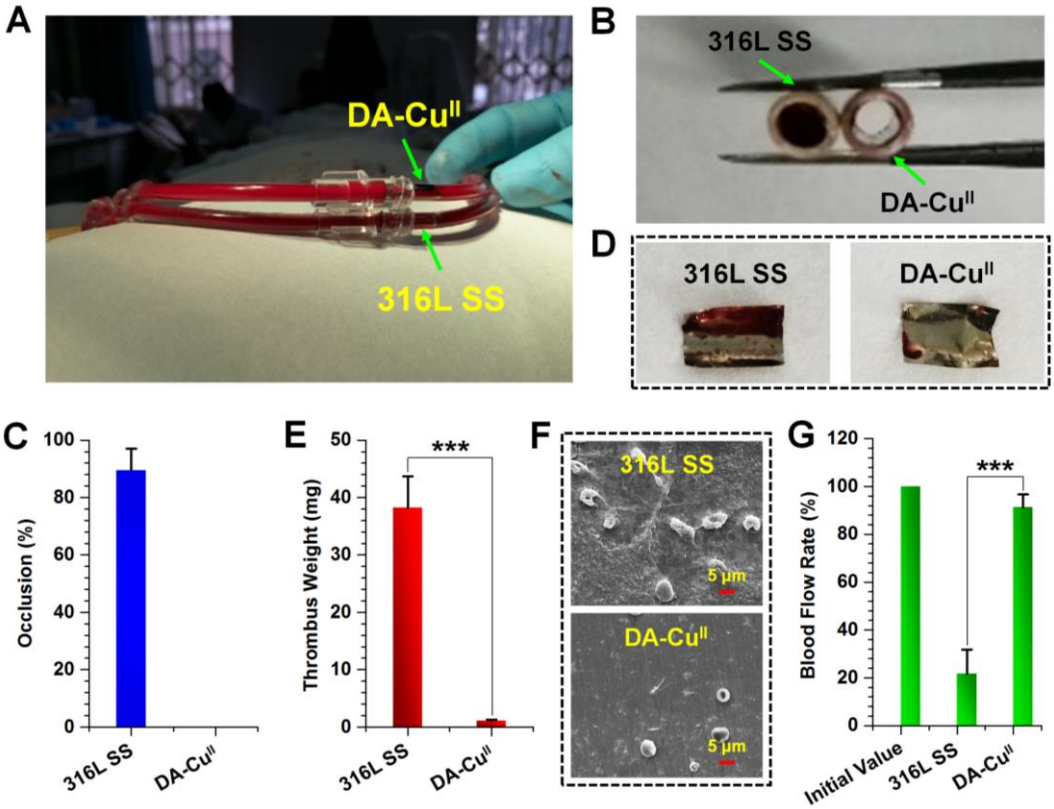

Fig. 7. Anti-thrombogenicity analysis of the DA-Cu^{II}-coated 316L SS foils. (A) Representative images of *ex vivo* AV-shunt model of a rabbit. (B) Cross-sectional photographs of tubes with internal installation of uncoated and DA-Cu^{II}-coated 316L SS foils after exposure to blood flow for 2 h. (C) The thrombus formed on the luminal surface of uncoated and DA-Cu^{II} coated 316L SS foils. (D) Occlusion percentage of the tube calculated by cross-sectional diameter. Please note the significant reduction in the occlusion after coating the foil surface with DA-Cu^{II} thin films. (E) Thrombus weight formed in different 316L SS circuits. (F) SEM images of platelets and fibrinogen on the surface of uncoated and DA-Cu^{II} coated 316L SS foils. (G) Blood flow rates in different tubing circuits at the end of extracorporeal circulation experiments. Data are presented as mean ± SD and analyzed by one-way ANOVA (***$p < 0.001$).

3.5 In vivo stent implantation

During the process of cardiovascular stent implantation, a stent is mounted onto an angioplasty balloon and dilated to desired target size. As a result, the stent undergoes a rigorous and complex distortion. Good coating adhesion strength and flexibility play key roles in withstanding stent deformation for the maintenance of the surface performance after stent implantation [23]. Thus, we performed a balloon dilatation test before the *in vivo* implantation experiment to investigate the mechanical behaviors of DA-Cu^{II} coating on the 316L SS cardiovascular stents. The SEM results demonstrated that the DA-Cu^{II} coating was still intact, homogeneous and continuous without any appearance of delamination or destruction after balloon dilatation, indicating that the DA-Cu^{II} coating is strong enough to endure the deformation of the 316L SS stent during the dilation procedure (**Fig. S9**).

We then performed *in vivo* implantation in a rabbit iliac artery replacement model to evaluate the feasibility of the DA-Cu^{II} coatings to promote re-endothelialization and suppress LSR and LST. The uncoated and DA-Cu^{II} coated 316L SS stents were collected after implantation for 1 and 3 months, and were then analyzed by SEM to examine endothelialization (**Fig. 8**). From the SEM images, we could observe that the luminal surface of the naked 316L SS stent was not fully covered with elongated ECs

after 1 month, while the DA-Cu^{II} coated stent surface was completely covered by a compact EC monolayer. After 3 months of implantation, the surface of the naked 316L SS stent showed little endothelial coverage, but a multitude of fiber-like tissues. In contrast, an intact endothelium with alignment along the blood stream was observed on the DA-Cu^{II} coated surface, indicating better re-endothelialization.

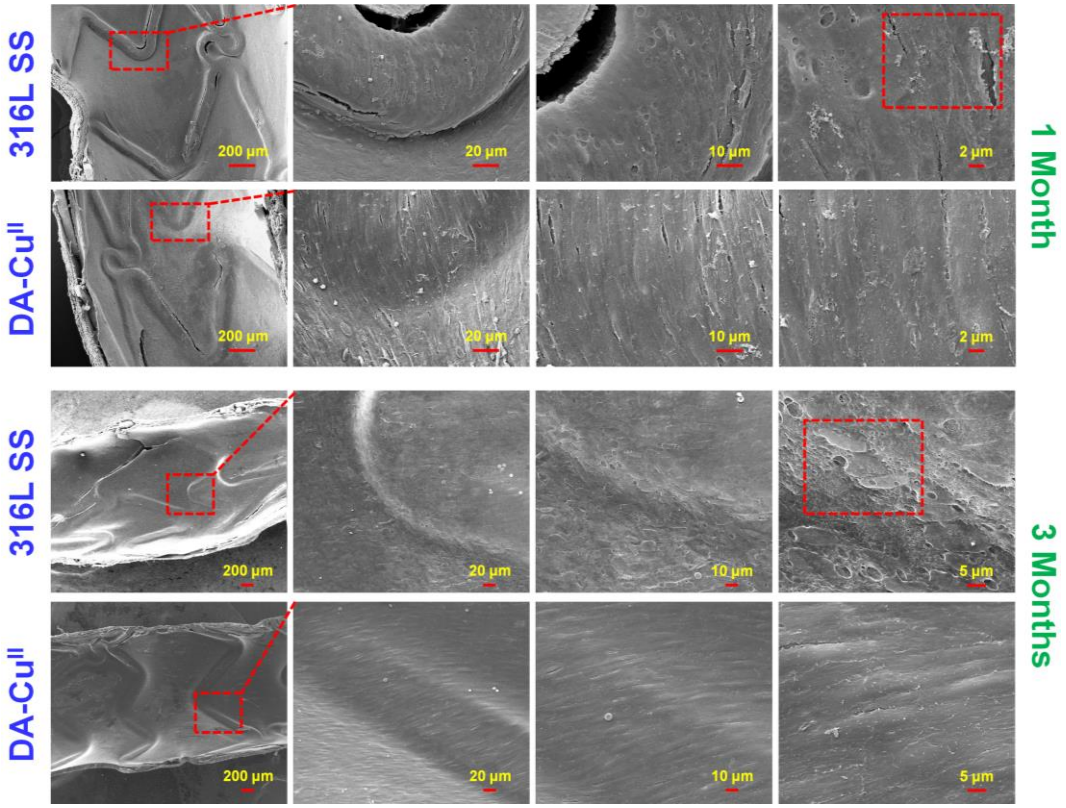

Fig. 8. Representative SEM images of cardiovascular stents modified by the DA-Cu^{II} coatings to enhance re-endothelialization after implantation for 1 and 3 months.

To further understand the effect of DA-Cu^{II} coatings on in-stent restenosis, we conducted a histomorphometric analysis with Van Gieson's staining (**Fig. 9**). The staining images showed that there was noticeably little neointimal hyperplasia percentage on the lumen of the DA-Cu^{II} coated 316L SS stents when compared to the control 316L SS stents after implantation for 1 or 3 months. Quantitative analysis revealed that both mean neointimal area and neointimal stenosis percentage were markedly reduced in the DA-Cu^{II} coated samples (1.5 ± 0.3 mm^2 and 11.5 ± 2.1 %) after 1 month when compared to the control 316L SS stents (3.2 ± 0.8 mm^2 and 25.2 ±

6.4 %) (**Fig. 9**B and C). After 3 months of implantation, despite that the mean neointimal area and stenosis percentage of the control 316L SS stents dramatically increasing to 6.4 ± 1.1 mm^2 and 41.5 ± 7.2 % respectively, there was only a small change in the DA-Cu^{II} coated samples (1.9 ± 0.4 mm^2 for the mean neointimal area, 13.2 ± 3.2 % for the neointimal stenosis percentage). Overall, these results from the *in vivo* experiment showed that the DA-Cu^{II} coated stents created a beneficial microenvironment to support stent re-endothelialization and achieved a physiological function of blood vessels. More importantly, it played a vital role in reducing in-stent restenosis to maintain long-term patency of the cardiovascular stents.

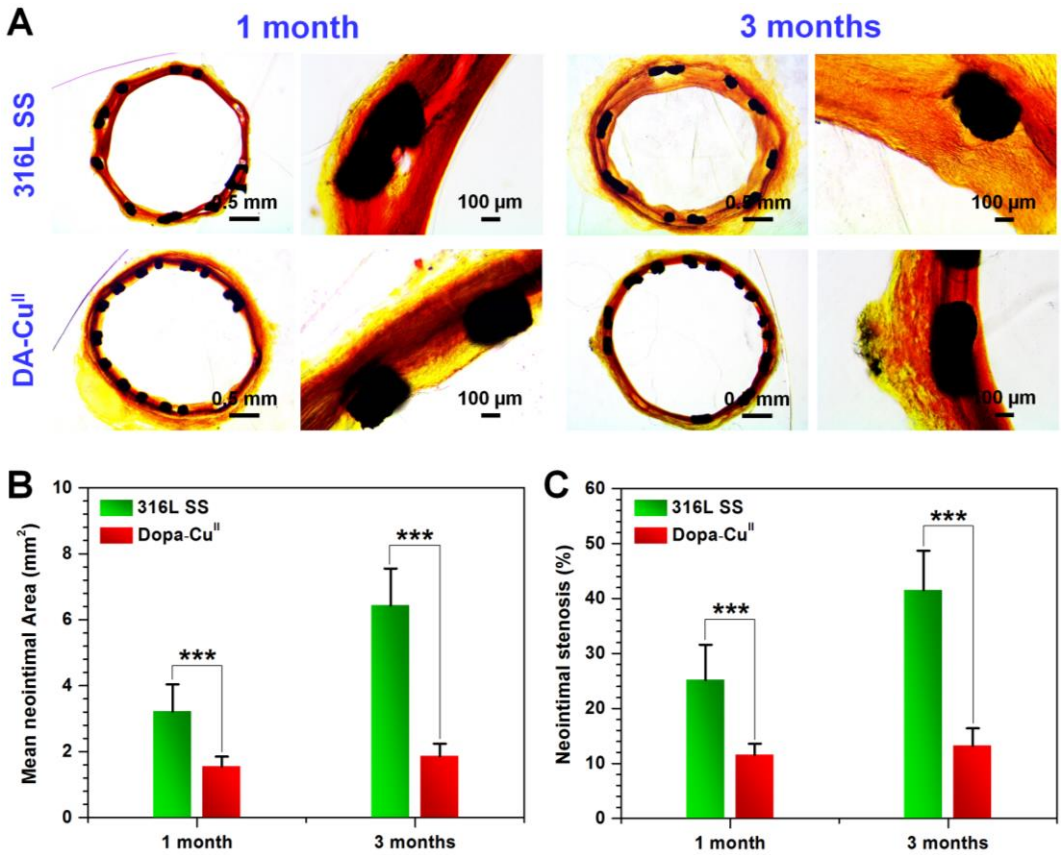

Fig. 9. Cardiovascular stents modified by the DA-Cu^{II} coatings to reduce in-stent restenosis. (A) The effect of uncoated and DA-Cu^{II}-coated 316L SS cardiovascular stents on restenosis evaluated by histomorphometric analysis after implantation for 1 and 3 months (n=4 for each time point). (B) Mean neointimal area and (C) neointimal stenosis percentage revealed that restenosis was considerably reduced after

modification of the stents with DA-Cu^{II}. Data are presented as mean ± SD, and analyzed by one-way ANOVA (***$p < 0.001$).

Although NO demonstrates numerous desirable physiological functions applied in the modification of vascular stents, its physiological functions are strongly dose dependent. An insufficient dosage of NO provided by vascular stents will not likely meet the demand of therapy, while an excessive dosage of NO can potentially cause a greater degree of interactions with superoxide to form peroxynitrites, leading to the harming of normal cells and tissue [42]. Therefore, a safe, controllable dose of NO generated from the stent surface is crucial to the success of stent implantation. NO-releasing and NO-generating materials are two representative types of materials which have been developed for surface modifying blood-contacting materials/devices. NO-releasing materials have been widely demonstrated and proposed that they are not suitable for application in long-term blood-contacting devices. This is due to the short half-lives of most NO donors which were used as prodrugs for fabricating NO-releasing materials and the unstable release of NO dosages (e.g. burst release of NO in the initial stage of implantation and insufficient dose of NO after implantation for 1 - 2 weeks) for *in vivo* applications [43-46]. The NO-generating materials, which can continuously, stably generate NO from their surfaces through the catalytic decomposition of S-RSNO into NO, are a promising application in long-term biomedical devices [22-24, 47, 48]. However, most of the existing strategies for constructing NO-generating materials usually involve complicated surface treatments or tedious multi-step processes [22, 23, 47, 48], thus limiting their practical application. Recently, we developed a mussel-inspired "one-pot" method to form an adhesive NO-generating coating on a 316 L SS stent-based one-step copolymerization of selenocystamine and dopamine (SeCA/DA) [24]. This "one-pot" method has unique advantages such as an environmentally friendly manufacturing condition, a simple manufacturing procedure, high stability, widespread practical applicability and no usage of organic solvents. Although the numerous advantages have been demonstrated by employing NO-generating coating of SeCA/DA,

it is subjected to its limited NO catalytic capability, with the biggest NO release rate being approximately 2×10^{-10} mol × cm^{-2} × min^{-1}. This value was less than the optimal physiological value (4×10^{-10} mol × cm^{-2} × min^{-1}) [20]. In consideration of an insufficient amount of NO leading to undesirable physiological functions, we further developed a one-step metal-catecholamine assembled strategy to prepare a durable in situ NO-generating biomimetic coating (DA-Cu^{II}). Using this new strategy, the obtained DA-Cu^{II} NO-generating coatings possessed an adjustable NO catalytic release rate of 0.4 to 6.5×10^{-10} mol × cm^{-2} × min^{-1}, which is comparable to the NO synthesis rate at physiological levels ($0.5 - 4 \times 10^{-10}$ mol × cm^{-2} × min^{-1}) [20]. It is noteworthy that we optimized the NO release rate which was suitable for EC growth, due to the much higher release rate of NO generated by the Cu^{II}-DA coating rather than SeCA-DA. This work serves as a guide for the design of an ideal NO-generating coating for improving anti-thrombogenicity, anti-restenosis as well as the endothelialization of vascular stents.

4. Conclusion

In this study, we have developed a facile "one-pot" surface modification approach to successfully prepare a tunable NO-generating coating onto cardiovascular stents. We used the method of dip-coating with an aqueous solution containing DA and Cu^{II}. The resultant DA-Cu^{II} coating exhibited effective catalytic decomposition of endogenous RSNOs in the circulating blood. Also, it enabled local, stable and long-term NO generation with a flux comparable to the physiological level produced by natural healthy ECs. In addition, *in vitro* cell studies demonstrated that such NO-generating coatings could selectively promote HUVEC attachment, migration and growth, while simultaneously inhibiting HUASMC adhesion, proliferation and migration. Moreover, we observed significant enhancements of the competitive adhesion and growth of HUVECs over HUASMCs on the DA-Cu^{II} coatings. The *ex vivo* anti-thrombogenic tests and *in vivo* implantation experiments further revealed that the DA-Cu^{II} coated stents with good mechanical properties not only inhibited platelet

activation/aggregation and thrombus formation, but also promoted re-endothelialization and reduced neointimal formation. In summary, this one-step surface modification strategy that prepares bio-inspired DA-Cu^{II} coatings offers the possibility to address major drawbacks of current BMS and DES technologies. Our strategy provides a native endothelium-mimetic microenvironment that supports rapid *in situ* re-endothelialization, and prevents long-term complications such as LSR and LST. Consequently, our surface modification strategy has great potential to be extensively applied in the field of blood-contacting devices.

Acknowledgements

This work was supported by the National Natural Science Foundation of China (Project 81501596, 31570957 and Key Program 81330031), the Distinguished Young Scholars of Sichuan Province (Project 2016JQ0027), the Fundamental Research Funds for the Central Universities (Project 2682018ZT23), and start-up fund (1-ZE7S) and central research fund (G-YBWS) from the Hong Kong Polytechnic University.

Appendix A. Supplementary data

Supplementary data related to this article can be found at.

References

[1] G.A. Roth, C. Johnson, A. Abajobir, F. Abd-Allah, S.F. Abera, G. Abyu, M. Ahmed, B. Aksut, T. Alam, K. Alam, Global, regional, and national burden of cardiovascular diseases for 10 causes, 1990 to 2015, J. Am. Coll. Cardiol. 70(1) (2017) 1-25.
[2] T. Palmerini, U. Benedetto, G. Biondi-Zoccai, D. Della Riva, L. Bacchi-Reggiani, P.C. Smits, G.J. Vlachojannis, L.O. Jensen, E.H. Christiansen, K. Berencsi, Long-term safety of drug-eluting and bare-metal stents: evidence from a comprehensive network meta-analysis, J. Am. Coll. Cardiol. 65(23) (2015) 2496-2507.
[3] C.C. Mohan, A.M. Cherian, S. Kurup, J. Joseph, M.B. Nair, M. Vijayakumar, S.V. Nair, D. Menon, Stable titania nanostructures on stainless steel coronary stent surface for enhanced corrosion resistance and endothelialization, Adv. Healthcare Mater. 6(11) (2017) 1601353.
[4] M. Alagem-Shafir, E. Kivovich, I. Tzchori, N. Lanir, M. Falah, M. Flugelman, U. Dinnar, R. Beyar, N. Lotan, S. Sivan, The formation of an anti-restenotic/anti-thrombotic surface by immobilization of nitric oxide synthase on a metallic carrier, Acta Biomater. 10(5) (2014) 2304-2312.

[5] C. Liang, Y. Hu, H. Wang, D. Xia, Q. Li, J. Zhang, J. Yang, B. Li, H. Li, D. Han, Biomimetic cardiovascular stents for in vivo re-endothelialization, Biomaterials 103 (2016) 170-182.
[6] K. Zhang, T. Liu, J.A. Li, J.Y. Chen, J. Wang, N. Huang, Surface modification of implanted cardiovascular metal stents: from antithrombosis and antirestenosis to endothelialization, J. Biomed. Mater. Res. A. 102(2) (2014) 588-609.
[7] Y. Wei, Y. Ji, L.L. Xiao, Q.K. Lin, J.P. Xu, K.F. Ren, J. Ji, Surface engineering of cardiovascular stent with endothelial cell selectivity for in vivo re-endothelialisation, Biomaterials 34(11) (2013) 2588-2599.
[8] G.C. Alexander, P.T. Hwang, J. Chen, J.-a. Kim, B.C. Brott, Y.-S. Yoon, H.-W. Jun, Nanomatrix coated stent enhances endothelialization but reduces platelet, smooth muscle cell, and monocyte adhesion under physiologic conditions, ACS Biomater. Sci. Eng. 4(1) (2017) 107-115.
[9] S. Takabatake, K. Hayashi, C. Nakanishi, H. Hao, K. Sakata, M.A. Kawashiri, T. Matsuda, M. Yamagishi, Vascular endothelial growth factor-bound stents: application of in situ capture technology of circulating endothelial progenitor cells in porcine coronary model, J. Interv. Cardiol. 27(1) (2014) 63-72.
[10] B. Gunasekera, C. Abou Diwan, G. Altawallbeh, H. Kalil, S. Maher, S. Xu, M. Bayachou, Functional Layer-by-layer thin films of inducible nitric oxide (NO) synthase oxygenase and polyethylenimine: modulation of enzyme loading and NO-release activity, ACS Appl. Mater. Interfaces 10(9) (2018) 7745-7755.
[11] M.A. Elnaggar, S.H. Seo, S. Gobaa, K.S. Lim, I.H. Bae, M.H. Jeong, D.K. Han, Y.K. Joung, Nitric oxide releasing coronary stent: a new approach using layer-by-layer coating and liposomal encapsulation, Small 12(43) (2016) 6012-6023.
[12] Z. Wang, Y. Lu, K. Qin, Y. Wu, Y. Tian, J. Wang, J. Zhang, J. Hou, Y. Cui, K. Wang, Enzyme-functionalized vascular grafts catalyze in-situ release of nitric oxide from exogenous NO prodrug, J. Controlled Release. 210 (2015) 179-188.
[13] Y. Farhatnia, A. Tan, A. Motiwala, B.G. Cousins, A.M. Seifalian, Evolution of covered stents in the contemporary era: clinical application, materials and manufacturing strategies using nanotechnology, Biotechnol Adv. 31(5) (2013) 524-542.
[14] A.W. Carpenter, M.H. Schoenfisch, Nitric oxide release: Part II. Therapeutic applications, Chem. Soc. Rev. 41(10) (2012) 3742-3752.
[15] A. de Mel, F. Murad, A.M. Seifalian, Nitric oxide: a guardian for vascular grafts?, Chem. Rev. 111(9) (2011) 5742-5767.
[16] M.C. Jen, M.C. Serrano, R. Van Lith, G.A. Ameer, Polymer-based nitric oxide therapies: recent insights for biomedical applications, Adv. Funct. Mater. 22(2) (2012) 239-260.
[17] A.B. Seabra, G.Z. Justo, P.S. Haddad, State of the art, challenges and perspectives in the design of nitric oxide-releasing polymeric nanomaterials for biomedical applications, Biotechnol Adv. 33(6) (2015) 1370-1379.
[18] N. Naghavi, A. de Mel, O.S. Alavijeh, B.G. Cousins, A.M. Seifalian, Nitric oxide donors for cardiovascular implant applications, Small 9(1) (2013) 22-35.
[19] Q. Wang, B. Akhavan, F. Jing, D. Cheng, H. Sun, D. Xie, Y. Leng, M.M. Bilek, N. Huang, Catalytic formation of nitric oxide mediated by Ti–Cu coatings provides

multifunctional interfaces for cardiovascular applications, Adv. Mater. Interfaces 5(6) (2018) 1701487.
[20] D.A. Riccio, M.H. Schoenfisch, Nitric oxide release: Part I. Macromolecular scaffolds, Chem. Soc. Rev. 41(10) (2012) 3731-3741.
[21] A.K. Winther, B. Fejerskov, M. Ter Meer, N.B. Jensen, R. Dillion, J.E. Schaffer, R. Chandrawati, M.M. Stevens, L.J. Schultze Kool, U. Simonsen, Enzyme prodrug therapy achieves site-specific, personalized physiological responses to the locally produced nitric oxide, ACS Appl. Mater. Interfaces 10(13) (2018) 10741-10751.
[22] Y. Weng, Q. Song, Y. Zhou, L. Zhang, J. Wang, J. Chen, Y. Leng, S. Li, N. Huang, Immobilization of selenocystamine on TiO2 surfaces for in situ catalytic generation of nitric oxide and potential application in intravascular stents, Biomaterials 32(5) (2011) 1253-1263.
[23] Z. Yang, Y. Yang, K. Xiong, X. Li, P. Qi, Q. Tu, F. Jing, Y. Weng, J. Wang, N. Huang, Nitric oxide producing coating mimicking endothelium function for multifunctional vascular stents, Biomaterials 63 (2015) 80-92.
[24] Z. Yang, Y. Yang, L. Zhang, K. Xiong, X. Li, F. Zhang, J. Wang, X. Zhao, N. Huang, Mussel-inspired catalytic selenocystamine-dopamine coatings for long-term generation of therapeutic gas on cardiovascular stents, Biomaterials 178 (2018) 1-10.
[25] C.W. McCarthy, R.J. Guillory, J. Goldman, M.C. Frost, Transition-metal-mediated release of nitric oxide (NO) from S-nitroso-N-acetyl-d-penicillamine (SNAP): potential applications for endogenous release of NO at the surface of stents via corrosion products, ACS Appl. Mater. Interfaces 8(16) (2016) 10128-10135.
[26] S. Jin, X. Qi, B. Zhang, Z. Sun, B. Zhang, H. Yang, T. Wang, B. Zheng, X. Wang, Q. Shi, Evaluation of promoting effect of a novel Cu-bearing metal stent on endothelialization process from in vitro and in vivo studies, Sci. Rep. 7(1) (2017) 17394.
[27] Y. Ding, L.T. Weng, M. Yang, Z. Yang, X. Lu, N. Huang, Y. Leng, Insights into the aggregation/deposition and structure of a polydopamine film, Langmuir 30(41) (2014) 12258-12269.
[28] P.N. Coneski, M.H. Schoenfisch, Nitric oxide release: part III. Measurement and reporting, Chem. Soc. Rev. 41(10) (2012) 3753-3758.
[29] Z. Yang, Q. Tu, M.F. Maitz, S. Zhou, J. Wang, N. Huang, Direct thrombin inhibitor-bivalirudin functionalized plasma polymerized allylamine coating for improved biocompatibility of vascular devices, Biomaterials 33(32) (2012) 7959-7971.
[30] X. Li, H. Qiu, P. Gao, Y. Yang, Z. Yang, N. Huang, Synergetic coordination and catecholamine chemistry for catalytic generation of nitric oxide on vascular stents, NPG. Asia. Mater. 10 (2018) 482-496.
[31] Q. Huang, Y. Yang, R. Hu, C. Lin, L. Sun, E.A. Vogler, Reduced platelet adhesion and improved corrosion resistance of superhydrophobic TiO2-nanotube-coated 316L stainless steel, Colloids Surf B Biointerfaces 125 (2015) 134-141.
[32] Z. Yang, Q. Tu, Y. Zhu, R. Luo, X. Li, Y. Xie, M.F. Maitz, J. Wang, N. Huang, Mussel-inspired coating of polydopamine directs endothelial and smooth muscle cell fate for re-endothelialization of vascular devices, Adv. Healthcare Mater. 1(5) (2012) 548-559.

[33] N. Naghavi, A. de Mel, O.S. Alavijeh, B.G. Cousins, A.M. Seifalian, Nitric oxide donors for cardiovascular implant applications, Small 9(1) (2013) 22-35.
[34] R. Luo, Y. Liu, H. Yao, L. Jiang, J. Wang, Y. Weng, A. Zhao, N. Huang, Copper-incorporated collagen/catechol film for in situ generation of nitric oxide, ACS Biomater. Sci. Eng. 1(9) (2015) 771-779.
[35] L. Li, Y. Xu, Z. Zhou, J. Chen, P. Yang, Y. Yang, J.a. Li, N. Huang, The effects of Cu-doped TiO_2 thin films on hyperplasia, inflammation and bacteria infection, Appl. Sci. 5(4) (2015) 1016-1032.
[36] A. Lutzke, J.B. Tapia, M.J. Neufeld, M.M. Reynolds, Sustained nitric oxide release from a tertiary s-nitrosothiol-based polyphosphazene coating, ACS Appl. Mater. Interfaces 9(3) (2017) 2104-2113.
[37] J.L. Wang, B.C. Li, Z.J. Li, K.F. Ren, L.J. Jin, S.M. Zhang, H. Chang, Y.X. Sun, J. Ji, Electropolymerization of dopamine for surface modification of complex-shaped cardiovascular stents, Biomaterials 35(27) (2014) 7679-7689.
[38] J. Yang, Y. Zeng, C. Zhang, Y.X. Chen, Z. Yang, Y. Li, X. Leng, D. Kong, X.Q. Wei, H.F. Sun, The prevention of restenosis in vivo with a VEGF gene and paclitaxel co-eluting stent, Biomaterials 34(6) (2013) 1635-1643.
[39] J.S. Beckman, W.H. Koppenol, Nitric oxide, superoxide, and peroxynitrite: the good, the bad, and ugly, Am. J. Physiol. Cell Physiol. 271(5) (1996) C1424-C1437.
[40] H. Chang, K.F. Ren, J.L. Wang, H. Zhang, B.L. Wang, S.M. Zheng, Y.Y. Zhou, J. Ji, Surface-mediated functional gene delivery: an effective strategy for enhancing competitiveness of endothelial cells over smooth muscle cells, Biomaterials 34(13) (2013) 3345-3354.
[41] Z. Yang, K. Xiong, P. Qi, Y. Yang, Q. Tu, J. Wang, N. Huang, Gallic acid tailoring surface functionalities of plasma-polymerized allylamine-coated 316L SS to selectively direct vascular endothelial and smooth muscle cell fate for enhanced endothelialization, ACS Appl. Mater. Interfaces 6(4) (2014) 2647-2656.
[42] M.W. Vaughn, L. Kuo, J.C. Liao, Effective diffusion distance of nitric oxide in the microcirculation, Am. J. Physiol. Heart Circ. Physiol. 274 (1998) H1705-H1714.
[43] J.M. Buergler, F.O. Tio, D.G. Schulz, M.M. Khan, W. Mazur, B.A. French, A.E. Raizner, N.M. Ali, Use of nitric-oxide-eluting polymer-coated coronary stents for prevention of restenosis in pigs, Coron. Artery Dis. 11(4) (2000) 351-357.
[44] J.H. Yoon, C.J. Wu, J. Homme, R.J. Tuch, R.G. Wolff, E.J. Topol, A.M. Lincoff, Local delivery of nitric oxide from an eluting stent to inhibit neointimal thickening in a porcine coronary injury model, Yonsei. Med. J. 43(2) (2002) 242-251.
[45] C.E. Lin, D.S. Garvey, D.R. Janero, L.G. Letts, P. Marek, S.K. Richardson, D. Serebryanik, M.J. Shumway, S.W. Tam, A.M. Trocha, D.V. Young, Combination of paclitaxel and nitric oxide as a novel treatment for the reduction of restenosis, J. Med. Chem. 47(9) (2004) 2276-2282.
[46] M. Kushwaha, J.M. Anderson, C.A. Bosworth, A. Andukuri, W.P. Minor, J.R. Lancaster, P.G. Anderson, B.C. Brott, H.W. Jun, A nitric oxide releasing, self assembled peptide amphiphile matrix that mimics native endothelium for coating implantable cardiovascular devices, Biomaterials 31(7) (2010) 1502-1508.

[47] W. Cha, M.E. Meyerhoff, Catalytic generation of nitric oxide from S-nitrosothiols using immobilized organoselenium species, Biomaterials 28(1) (2007) 19-27.
[48] T.C. Major, D.O. Brant, C.P. Burney, K.A. Amoako, G.M. Annich, M.E. Meyerhoff, H. Handa, R.H. Bartlett, The hemocompatibility of a nitric oxide generating polymer that catalyzes S-nitrosothiol decomposition in an extracorporeal circulation model, Biomaterials 32(26) (2011) 5957-5969.